Gong et al. Future Cities and Environment (2015) 1:12
DOI 10.1186/s40984-015-0012-9

Future Cities & Environment
a SpringerOpen Journal

TECHNICAL ARTICLE Open Access

Photocatalytic degradation of high ammonia concentration wastewater by TiO_2

Xue Gong[1], Haifeng Wang[1], Chun Yang[1], Quan Li[1], Xiangping Chen[2] and Jin Hu[3*]

Abstract

This study explored the effect on photocatalytic degradation in aqueous solution with high- concentration ammonia where immobilized TiO_2 on glass beads was employed as the photocatalyst. TiO_2 film was prepared via deep coating TiO_2 in a sol–gel system of tetrabutyl titanate precursor and calcinating it at the temperature between 400 to 650 °C. Several crucial factors affecting on the rate of removal of ammonia were investigated. These factors included annealing temperature, catalyst composition, coated times of TiO_2 film, aqueous initial pH, UV exposure time, repetitions times, etc. The results validate the effectiveness as TiO_2 glass beads was employed for photocatalytic degradation treatment in high concentration ammonia solutions.

Keywords: Ammonia, Glass beads, TiO_2, Photocatalytic

Introduction

Early examples of research into the cleaning properties of TiO_2 include those carried out by Frank and Bard. They found that TiO_2 powder in contaminated water were able to photocatalyze the conversion of cyanide into cyanate and thus detoxified the water [15, 16].

One of the advantages of TiO_2 photocatalysis for water decontamination is that only the TiO_2 photocatalyst (immobilized or suspended) and UV light, either from solar light or artificial light sources, are needed and its cost can thus be lower than other kinds of advanced oxidation techniques (UV/O_3; $UV = H_2O_2$, photo-Fenton). Moreover, no toxic intermediate products are generated in the photocatalytic decontamination process. As a result, TiO_2 photocatalysis has been attracting a lot of interest in the areas of water detoxification or drinking water purification [6, 9, 36].

The main potentially-polluting nutrients in relation to water are nitrogen, ammonia, phosphorus and sulphur. Ammonia is a common water contaminant that has notable effects upon the environment and human health when it is in the presence of excess amounts. They arise from the natural breakdown of crop residues and soil organic matter, rainfall, wastewater and industrial effluents…etc. Free ammonia (NH3) and ionized-ammonia (NH4+) represent two forms of reduced inorganic nitrogen. The free ammonia is a gaseous chemical, whereas the NH4+ in the reduced nitrogen form exists in ionized form and remains soluble in water [40]. Ammonia is one of the key matters causing eutrophication pollution. Ammonia brings injurious effects on human and animal health in forms of gas and particle phase [2, 3].

In most cases, contamination of groundwater by chemicals derived from urban and industrial activities, modern agricultural practices, or waste disposal takes place almost imperceptibly. The concentration of nitrogen of the regional groundwater rises along with over fertilization in agriculture [1, 23, 45]. Solid waste produced by both municipal and industrial sectors increased the organic, heavy metals, and inorganic groundwater ions [34, 41, 49]. Excess discharge of domestic and industrial wastewater has also polluted the groundwater [32]. In general, ammonia level in ground waters is below 0.2 mg per litre. Higher natural contents (up to 3 mg/litre) are found in strata rich in humic substances, iron or in forests [12]. Surface waters may contain up to 12 mg/litre [4]. Ammonia may be present in drinking-water as a result of disinfection with chloramines. The maximum limit of ammonia set by the

* Correspondence: jin.hu@heig-vd.ch
[3]Institute of Thermal Engineering, University of Applied Sciences and Arts of Western Switzerland, Yverdon-les-Bains, Switzerland
Full list of author information is available at the end of the article

European Association for drinking water is approximately 0.5 mg/l (AWWA, [5]).

Currently, the most popular treatments for ammonia removal from wastewater are air stripping, ionic exchange and nitrification denitrification techniques where however, ammonia cannot be removed completely in most cases. For this reason in the recent years advanced oxidation processes have been investigated as the alternatives to conventional water treatment. [29] used the photocatalytic reduction method of Pt / TiO_2 nano-photocatalysts with high platinum loading of 0.5 % to achieve the best efficiency of nitrogen removal. [47] conducted TiO_2 photocatalyst doped with metal ions for treating ammonia nitrogen wastewater from coal gasification process. The ammonia nitrogen removal rate was approximately 79 %. Songhua River water treatment using catalyzed ozonation were investigated by [50]. In these cases, Nano TiO_2 coated haydite, silica-gel and zeolite were used as the catalyst. The ammonia removal efficiency was close to 80 % after 30 min reaction.

Typically, the studies with respect to photocatalytic reactors adopted either TiO_2 powder or suspended counterpart in the water being treated and then went through further process to remove the TiO_2. The primary aim of doing so is to avoid the post separation difficulties associated with the powder form of the TiO_2 catalyst. Immobilization of TiO_2 on various substrates is an important issue in the water treatment applications associated with photocatalytic technologies [43]. There are several advantages in these researches, including higher surface area, superior adsorption properties [24, 53], surface hydroxyl groups increase, and charge recombination reduction [46] in immobilized systems.

This study attempted to implant immobilized TiO_2 onto the small glass beads which were placed into the photocatalytic reactor to investigate and analyze its performance of treating ammonium-rich wastewater. Moreover, we aim to develop a simple, energy efficient, less expensive to build and operate photocatalytic reactor to handle ammonium-rich wastewater. This low cost solution will provide effective and successful experiences for large-scale industrial applications in the future.

Experimental setup and procedure

Experimental apparatus

Experimental apparatus is shown in Fig. 1; it mainly consists of an inner tube and outer borosilicate glass reactor of 500 mL capacity. The inner tube is equipped with a UV lamp (Xin Guang Yuan Lighting, 36 W, with an emission spectrum of 200–600 nm, and λ_{max} at 365 nm), which was mounted axially in the reactor inside a cylindrical, double walled lamp jacket. Instead of ordinary, the glass lamp jacket is made of quartz glass in order to reduce the absorption of ultraviolet light. The outer glass reactor as a photocatalytic reactor is to accommodate the inner tube where TiO_2 coated glass beads as the photocatalytic constituent, also as the aqueous samples were placed in. In this study, UV protective enclosure was used to bring out protection effect against exposure to UV radiation.

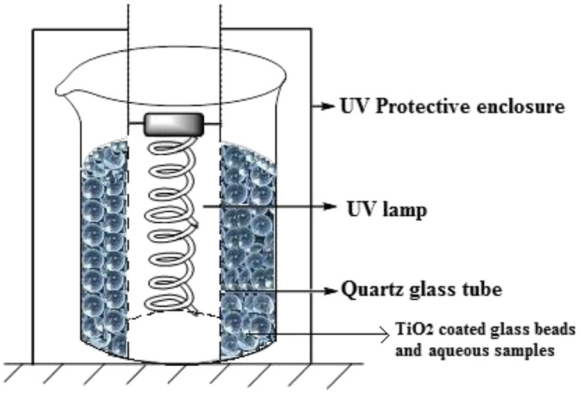

Fig. 1 Experimental apparatus: schematic of setup

TiO_2 thin film preparation

The TiO_2 films were prepared via sol-gel process. Fig. 2 illustrates this procedure in detail. Tetrabutyl titanate ((C4H9O) 4Ti) was used as a precursor to prepare TiO_2 sol. CH3CH2OH, ((HOCH2CH2)3 N) and distilled water were added to ((C4H9O) 4Ti) under continuous magnetic agitation at room temperature to form a mixture according to volume ratio of 3: 12: 1: 1. All chemicals used for this study were of analytical grade and from Chengdu Kelong Chemical Co., Ltd. Taking their high mechanical and chemical stability into account, this study selected the glass beads (diameter 5 mm) from Yongqing Ziguang Glass Beads Co., Ltd, as the substrate to be coated with nano-TiO_2. Before coating, the glass beads were etched for 24 h in diluted hydrofluoric acid and subsequently were sonicated (DH-120DT, Shanghai Dihoo Instrument) in acetone, absolute ethanol and distilled water for 10 min in order to remove all the organic contaminants. After that, they were dried out at 100 °C by DZF-6050 vacuum dryer (Shanghai Jinghong Laboratory Instrument).

TiO_2 thin films were deposited on glass slides by dip coating method at two different vertical withdrawal speeds of 1 cm/min. TiO_2 films were deposited several layers on substrates. During successive coatings, each layer was applied vacuum drying process for 30 min at 100 °C. After multiple dip coating was finished, the films were annealed at various temperatures in the range of 400 ~ 650 °C for 2 h at the heating rate 6 °C/min in an atmosphere.

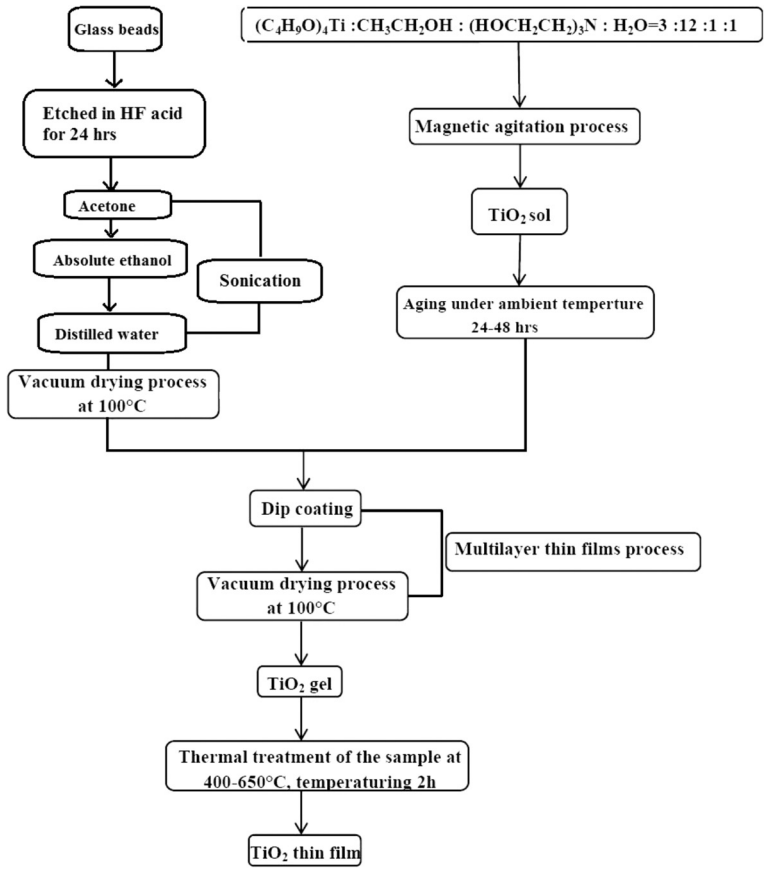

Fig. 2 The process of fabrication of TiO_2 thin films

Determination of the analyte concentration in a solution after degradation

In this study, the Beer–Lambert law was applied to predict the linear relationship between the absorbance of the solution and the concentration of the analyte (assuming all other experimental parameters invariant). A series of ammonium chloride NH_4Cl standard solutions were prepared. The absorbance of NH_4Cl for various concentrations was measured with a UV-vis spectrophotometer (Shanghai Puyuan Instrument) at a wavelength 425 nm, which offered an effective way to engender a calibration curve to show the absorbance variation along with the concentration as shown in Fig. 3. The slope and the intercept of the line provided a relationship between absorbance and concentration:

$$A = slope\ c + intercept \tag{1}$$

Experimental procedures followed this way: the process began with degradation before 300 ml aqueous sample was added to the outer container. The UV light was then turned on to start UV photolysis for a period of time. The absorbance of the sample was re-measured when the experiment was over. The degradation rate can be calculated with:

$$\eta = \frac{A_0 - A}{A_0} \times 100\% = \frac{C_0 - C}{C_0} \times 100\% \tag{2}$$

Where η represents degradation rate; A_0 represents the initial absorbance of the solution sample; A represents absorbance of the solution sample after a certain time of photocatalytic reaction; C_0 represents the initial concentration of solution sample; C represents the concentration of solution sample after degradation.

To ensure reproducibility and decrease the uncertainty, each measurement was repeated 3 times to take the average value. The nonlinear regression analysis was performed to best-fit the response function (photocatalytic degradation efficiency) with the actual experimental data.

Results and discussion

Structural properties of TiO_2 thin film

To determine the intrinsic properties of the TiO_2 layers, various techniques were used. X-ray diffraction (XRD,

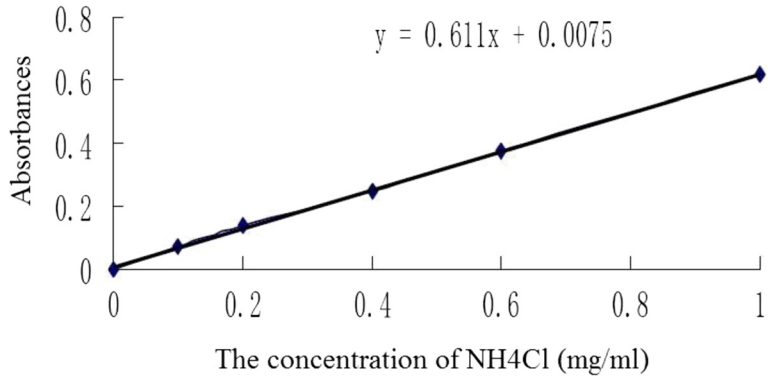

Fig. 3 The standard/calibration curve of absorbance for different concentrations of NH4Cl

model D8 ADVANCE, Bruker. Ltd) analysis of the films on the glass bead substrate was performed to determine the crystalline phase and to estimate the amendment of TiO_2 as heating temperature varied. The XRD patterns were recorded by step scanning in the 2θ scan range of 5–80° where a step size was of 0.01°. In Fig. 4, anatase phase and rutile phase are denoted as A and R, respectively.

Before heat treatment, the TiO_2 thin layer consisted of amorphous or poorly crystallized oxide. Figure 4 shows the XRD patterns of the TiO_2 films annealed at various temperatures. The line at 400 °C shows a prominent anatase peak at 25.4° (101) due to the transition from the amorphous phase to the anatase phase. When the calcined temperature increased to 450 °C, the crystallinity of TiO_2 was improved but still stayed on the anatase phase. As the temperature increased from 400 to 600 °C, there was significant growth for the intensities peaks, which revealed the improvement of the crystallinity. And the outcomes are in agreement with the finding demonstrated by Hasan et al. [19]. When temperature went up to 500 °C, the XRD pattern exhibited a rutile peak at 27.4° (110). At this temperature, it is thought that the transformation from anatase to rutile took place. Anatase/rutile mixture phase appeared when the TiO_2 thin film was annealed at 500 °C. At 600 °C, the rutile (110) peak went higher while the counterpart of the anatase (101) dropped. As far as the line of 650 °C, the anatase peak disappeared while the the rutile peak increased considerably, indicating that a complete transformation from the anatase phase to the rutile phase occurred. This phenomenon is in compliance with the work done by [26, 51]. They revealed that TiO_2 thin films can be transformed from amorphous phase into

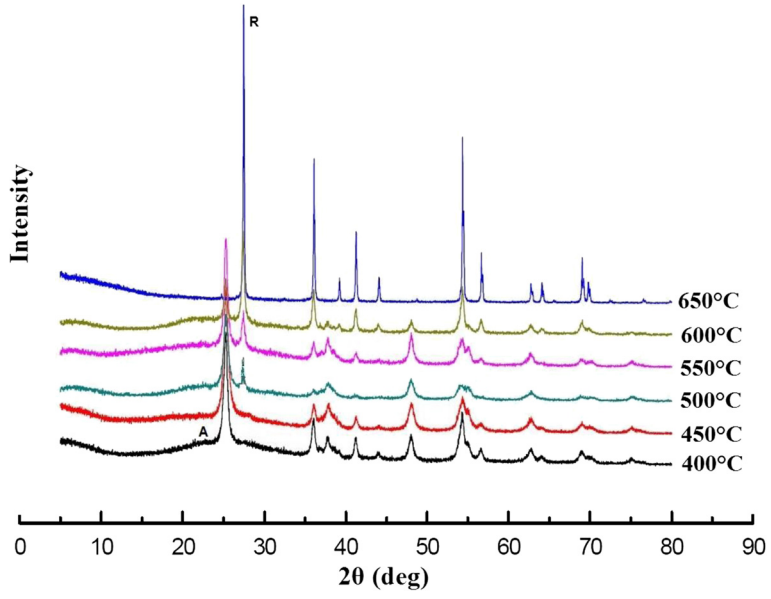

Fig. 4 XRD patterns of the TiO_2 films at various calcination temperatures

high degree crystalline anatase and then converted into rutile by temperature treatment. At above 600 °C, x-ray diffraction pattern showed a peak belonging to the rutile peak. Transformation from anatase to rutile is thought to occur at about 500 °C with the complete transformation at higher temperature. The average crystallite sizes of the samples were estimated by the Debye–Scherrer's equation as expressed below:

$$\text{Crystallite size}, D = 0.9\lambda/\left(\beta_{hkl}\cdot \text{Cos}\ \theta_{hkl}\right) \quad (3)$$

where D is the diameter of crystalline in nm, λ is the X-ray wavelength of Cu Kα radiation, β_{hkl} is broadening of the hkl diffraction peak width at half height of the maximum intensity (FWHM) in radians and θ_{hkl} is the diffraction angle (Bragg's angle) in degrees.

For TiO_2 thin films that contain anatase and rutile phase only, the percentage of mass fraction (X_A) for anatase phase in the solution was calculated using the relative intensity of maximum peak of anatase phase (101) and a maximum peak of rutile phase (110). The X_A is expressed by the equation below [44];

$$X_A = \frac{1}{1 + 1.265\frac{I_R}{I_A}} \quad (4)$$

Where X_A, I_A, I_R refer to a contents of the anatase phase in the solutions, the intensity at the anatase phase peak as well as the intensity at rutile phase peak, respectively. Meanwhile, the constant 1.265 is the scattering coefficient [54]. The rutile weight fraction X_R can be calculated by the empirical equation as followed [38]:

$$X_R = \frac{1}{1 + 0.8\frac{I_A}{I_R}} \quad (5)$$

The influent factors associated to annealing temperature on the structure of TiO_2 were summarized in Table 1. As the table has shown, annealing temperature rise results in bigger crystallite size. For instance, when the annealing temperature increased from 400 to 600 °C, the crystallite size on of anatase phase grew from 14.4 to 18.72 nm. Similarly, the crystallite size of rutile phase grew from 37.06 nm to 67.94 nm with the increasing of annealing temperature from 500 to 650 °C. It is observed that the X_A of anatase phase was 86.31 % and it decreased to 26.92 % as the annealing temperature increased from 500 to 600 °C. It is noticeable that the amount of rutile phase increased with annealing temperature rise from 500 to 650 °C.

TiO_2 exists in the form of three polymorphs: anatase, rutile, and brookite [11]. Although rutile phase has less photocatalytic activity than anatase, Anatase/rutile mixture phase is known to exhibit enhanced photoactivity relative to single-phase titania [13, 21, 37, 42, 48]. It is widely recognized that this is a result of improved charge carrier separation, possibly through the trapping of electrons in rutile and the consequent reduction in electron–hole recombination [8, 21]. Anatase-to-rutile phase transformation is governed by the annealing temperature, compactness of the anatase nanocrystallites, and grain boundary defects [28, 30].

The influence of exposure time on the TiO_2 films under UV irradiation

Over the trail test, TiO_2 thin films were categorized into 4 groups based on their anneal temperatures of 450 °C, 500 °C, 550 °C and 600 °C under UV irradiation. Comparison among the 4 groups was conducted to check the influence of exposure time on ammonia degradation rate. Ammonia content of wastewater was about 700 mg / L. The volume of reaction solution was 300 ml. The solution was adjusted to a pH of 7. The degradation was carried out at room temperature. The photocatalytic reaction time was 30, 60, 90, 120 and 150 min, respectively. The results are shown in Fig. 5.

The results from Fig. 5 indicate that the photocatalytic activities/degradation rate of the thin TiO_2 films prepared at 4 different temperatures displayed the same pattern in function of UV exposure time. As shown in Table 1, TiO_2 presented photocatalytic activity on anatase phase without

Table 1 The influence of temperature on the grain size and content of TiO_2 thin film

T (°C)	Phase	K	λ (nm)	β (radian)	*cosθ*	hkl	D (nm)	Mass ratio (%)
400	Anatase	0.89	0.154	0.009546	0.997	101	14.40407	100
450	Anatase	0.89	0.154	0.995986	0.996	101	14.71318	100
500	Anatase	0.89	0.154	0.997976	0.998	101	15.11035	86.31
	Rutile	0.89	0.154	0.4324127	0.432	110	37.06334	9.04
550	Anatase	0.89	0.154	0.998008	0.998	101	15.79999	72.88
	Rutile	0.89	0.154	0.417477	0.417	110	45.66140	18.87
600	Anatase	0.89	0.154	0.998589	0.998	101	18.72492	26.92
	Rutile	0.89	0.154	0.435115	0.435	110	48.12791	62.98
650	Rutile	0.89	0.154	0.385424	0.385	110	67.94198	100

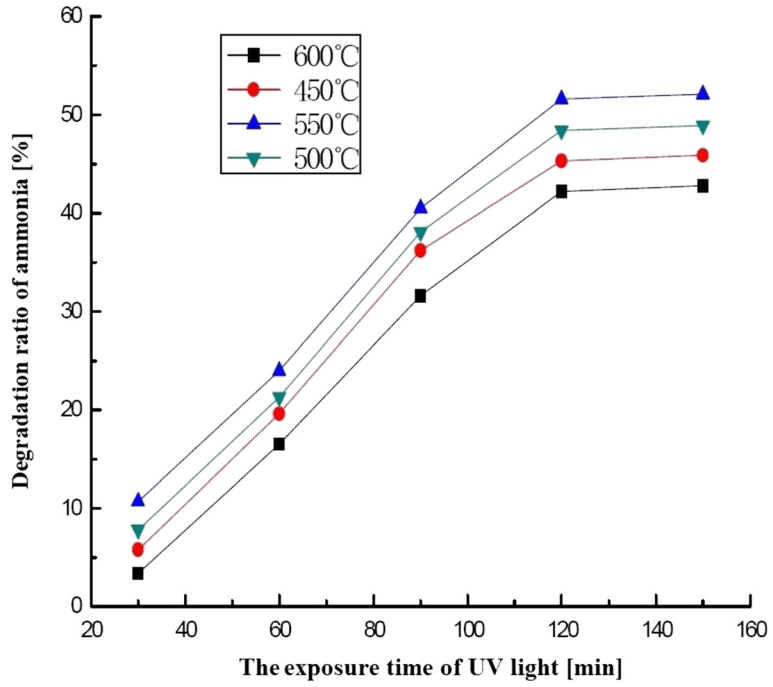

Fig. 5 The influence of exposure time of the TiO_2 films under UV irradiation on ammonia degradation rate

phase conversion at 450 °C. Anatase/rutile mixture phase was seen at 500 °C. At this temperature, anatase is converted to rutile with 9.04 % rutile phase in the mixed phase. This mixed phase has higher photocatalytic activities than single anatase phase. When the sample was prepared at 550 °C (Rutile 18.87 %, Anatase 72.88 %), which has the highest photocatalytic activity among all thin films tested. Sample annealing at 600 °C resulted in 62.98 % rutile phase as a predominantly phase in the mixed phase. At this temperature, TiO_2 thin film displayed much less photocatalytic activity than other 3 samples. Ding et al [14] conducted the degradation of organic dye solution using mixed crystal nano TiO_2 as a photocatalyst. They found the photocatalytic activity of mixed phase nano-TiO_2 crystal samples was significantly higher than that of a single crystal sample or mechanical mixed crystal samples. The photocatalytic activities had the best effect when the mass fraction of rutile phase was about 20 % of mixed crystals. Ji et al [22] prepared anatase - rutile mixed Nano TiO_2 crystal samples to test degradation effect of Methyl orange solution. They found when rutile phase is of 18.9 % of mixed crystal, the photo degradation rate of methyl orange can reach the highest 85 %. Degussa P-25 (a mixed-phase titania photocatalyst) is commercially available and was utilized as a reference material in many studies. This nanocrystalline material, formed by flame pyrolysis, consists of 80 wt% anatase and 20 wt% rutile. Our experimental results were in good agreement with other authors' findings described above.

As can be seen from Fig. 5, over UV exposure time from 30 to 120 min, it is evident that the percentage of photo-degradation for the four samples increases along with irradiation time growth. After 120 min, the growth of the degradation rate of all samples substantially slowed down and almost ceased. This could be attributed to the following reason: in general, the photoactivity of TiO2 is determined by the processes of electron/hole pair generation, recombination, interfacial transfer and by the surface reactions of these charge carriers with the species adsorbed on the surface of the photocatalyst [[10, 17, 18, 31]]. The presence of molecular oxygen in the solution also plays a substantial role in the photo-induced processes on irradiated TiO2 surfaces because that it enables an effective charge carriers separation. Consequently, both superoxide radical anion and hydrogen peroxide as the most important products of the molecular oxygen reduction play an important role in the complex mechanism of Oxygen Species (ROS, e.g., •OH, •O2H or singlet oxygen) generation on the irradiated TiO2 surfaces [[20, 31, 35, 52]]. Hydroxyl radicals are powerful and indiscriminate oxidizing species. The redox reactions at the surface of the particles lead to the generation of active oxygen species which can attack organic and inorganic species at or near the surface. However, the photocatalytic degradation of ammonia will lead to generate significant number of intermediates species in the reaction mixture which can't be removed efficiently in the reactor. They gradually accumulated and eventually

deposited on the TiO_2 film surfaces around reaction time of 2 h which deactivate the active sites and reduce the hydroxyl radicals and active oxygen species generation on thin film surface who play an important role in oxidizing.

The influence of TiO_2 layer coated times on ammonia degradation rate

In order to obtain multilayer thin films with controllable thickness, 1-10 TiO_2 layers were successively coated on glass beads using dip-coating steps and then thermally treated as aforementioned process.

The photocatalytic degradation of ammonia in water was conducted respectively with the glass beads coated with 1 to 10 layers of TiO_2 thin film. The ammonia concentration in wastewater was about 700 mg / L, initial pH of wastewater sample was 7; the degradation was at room temperature for 120 min.

It is clearly seen from Fig. 6 that under the same experimental conditions, the degradation efficiency depends on the film thickness. It was found that the degradation efficiency increased with both TiO_2 film layers and film thickness growth but not linearly dependent. It is most likely that more titanium dioxide participated in the photocatalytic reaction. However, the growth of the degradation efficiency over 6 times of coating seemed to slow down or even stayed on the same level while the first 6 coatings greatly improved the degradation efficiency.

Figure 6 implies that we cannot achieve greater degradation efficiency by unlimited increasing coating layers or film thickness. An optimum value of TiO_2 film thickness is presented. Jin et al. [25] showed the transmission spectra of the TiO_2 films with various coating times. They demonstrated that the transmittances of the TiO_2 thin films coated 5 times and 15 times were higher than that of the thin film coated 30 times in the visible range of 400 nm ~ 800 nm. Moreover, photocatalytic chemical reactions occurred on the surface of TiO_2 thin films. Meanwhile, titanium dioxide in the interior region of thin films was not easy to contact the reactant and reaction products were also not easy to enter the solution. Therefore, the photocatalytic activity of titanium dioxide in the interior region of thin films was lower than that of titanium dioxide in the surface of thin films.

The surface topography and the microstructure of the coatings were examined by scanning electron microscopy (SEM). The film thickness was measured by using SEM and weight methods.

Fig. 7a showed that the glass beads surfaces presented inhomogeneous surfaces after two times coating without full coverage of nanoparticles to provide more reaction sites on the surface over the photocatalytic reaction. Nanoparticles are in irregular shapes and majority of the nanoparticles formed into a monolayer with a few bare or multilayered patches. The film thickness is ~230 nm. Fig. 7b illustrated that the layer consisting of four films yielded totally smooth surface. The full coverage of nanoparticles was observed. When the coating became thicker, it became denser. The film thickness is ~410 nm. The surface particles are in good contact with low surface roughness. Fig. 7c revealed that the surface of the six films layer appeared to be wrinkled while the good crystallinity and homogeneous nanostructure surface area were obtained after the 6 times of coating. Both the boundaries between particles

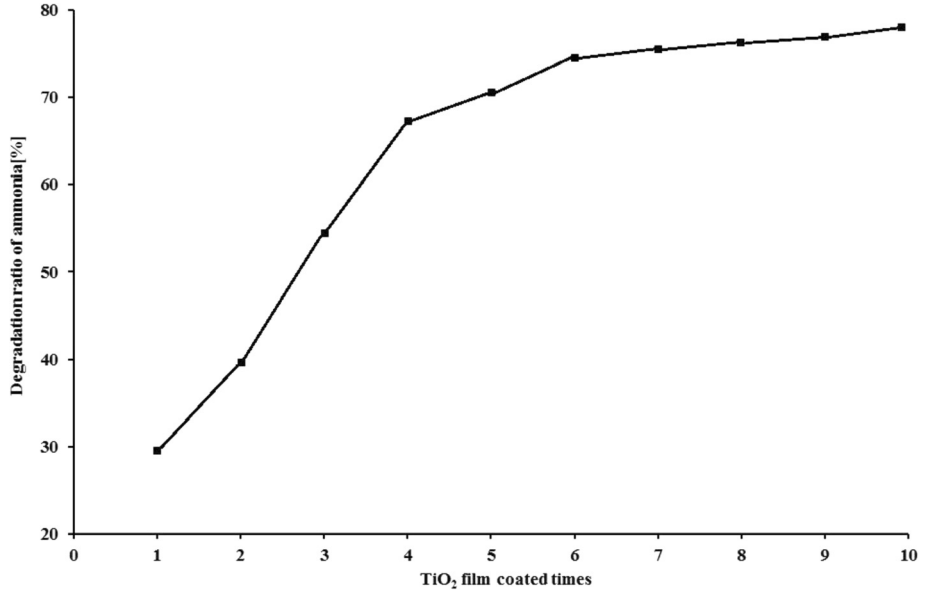

Fig. 6 TiO_2 film coated times as function of degradation efficiency

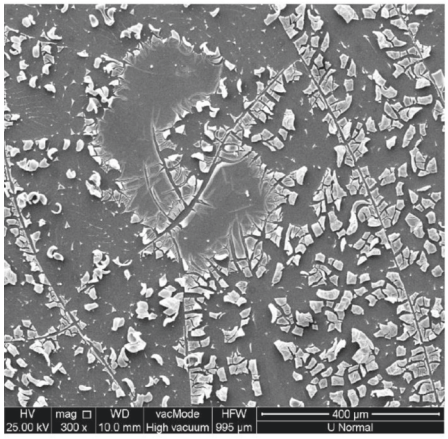

a SEM photograph of 2 layers nano TiO_2 thin films

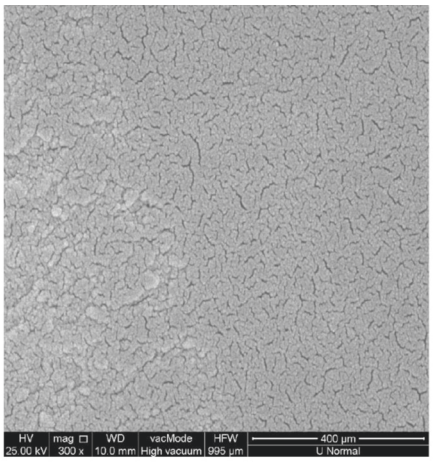

b SEM photograph of 4 layers nano TiO_2 thin films

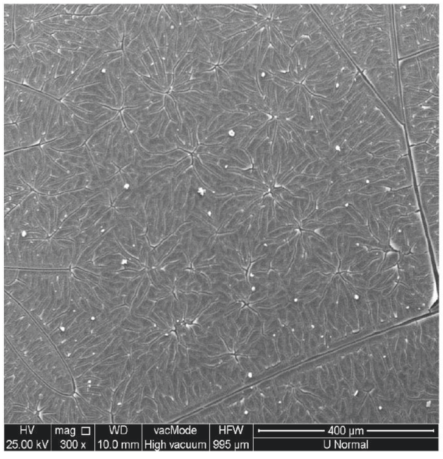

c SEM photograph of 6 layers nano TiO_2 thin films

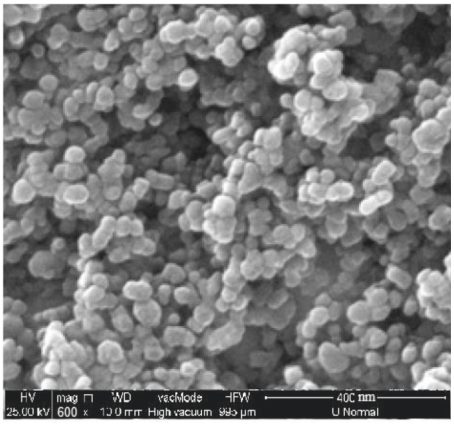

d SEM photograph of 10 layers nano TiO_2 thin films

Fig. 7 SEM images of (**a**) 2 (**b**) 4 (**c**) 6 and (**d**) 10 layers of TiO_2 thin film

and the grain sizes were clearly observed. These surface particles were in close contact and they formed the blocks with higher density where the film thickness is ~570 nm. Fig. 7c suggested a link between the grain size growth and the increase in roughness. Fig. 7d provided the image of the surface of ten layers films under higher magnification. The surface particles were piled up in layers and the grains agglomeration formed clusters. The film thickness is ~900 nm.

The influence of aqueous initial pH on degradation efficiency

The pH condition has been reported to affect the photocatalytic reaction rate. Before turning on the UV lamp, the pH of the aqueous solution was adjusted to the desired value by dropwise addition, 0.5 mol HCl solution or NaOH solution (Chengdu Kelong Chemical Co., Ltd). The concentration of ammonia was about 700 mg/L. The suspension was placed in the dark, shielded with aluminum foil and stirred until the pH stable.

The degradation efficiencies of ammonia in aqueous wastewater during UV illumination for pH from 1 to 13 were investigated as presented in Fig. 8. It was observed that the initial pH values of water samples had significant impacts on the photocatalytic degradation rate. In the pH range 1 – 3.4, the photocatalytic degradation efficiency increased with time. pH =3.4 had the maximum degradation of ammonia, removal efficiencies of ammonia in wastewater were above 70 %. When pH values exceeded 3.4, the photocatalytic degradation rate decreased dramatically. It is concluded that the overall degradation rate under strong acidic or mildly acidic were higher than those under neutral or mildly alkaline or strongly alkaline conditions. The possible reason is

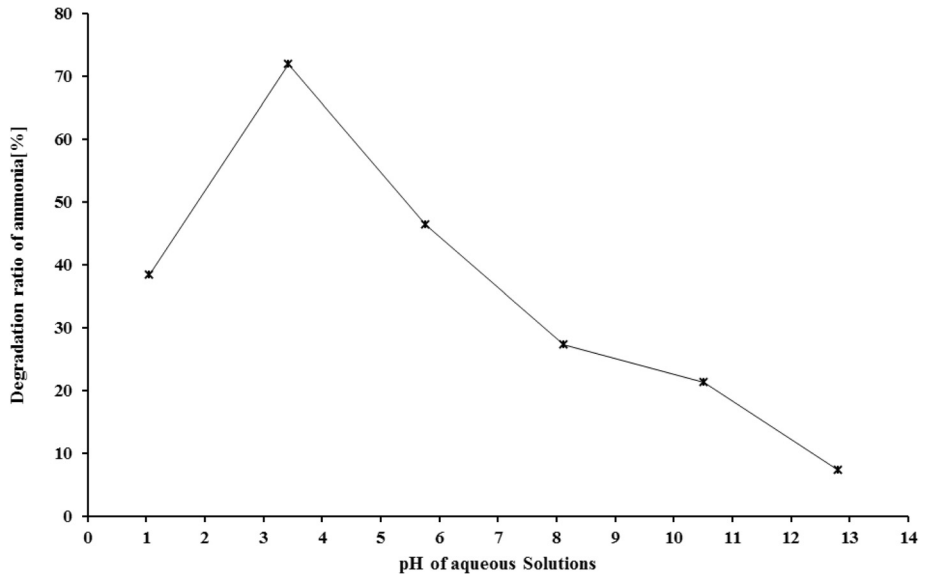

Fig. 8 Relationship between aqueous initial pH and degradation efficiency

that the surface charge of TiO_2 particles was influenced by the pH value in the solution. [7] already reviewed that acid-base properties of the metal oxide surfaces could considerably affected their photocatalytic activity. The point of zero charge (pzc) of the TiO_2 (Degussa P25) was at pH 6.8 [39]. Thus, the TiO_2 surface was positively charged in acidic media (pH < 6.8), whereas it is negatively charged under alkaline conditions (pH > 6.8). At the acidic condition, TiO_2 surface was positively charged while the wastewater contained negatively charged groups to improve the absorbance and the photocatalytic effect. In contrast, Sun et al. [47] suggested that the ammonia removal rate was larger in the alkaline condition than that in acidic condition. He also pointed out that an optimum removal rate was obtained at pH 9.1 when the concentration of ammonia was 546 mg/L. Murgia et al. [33] carried out a kinetic study of photo oxidation over TiO_2 of NH3/NH4 in the high concentration range of 26 – 214 mg/l. They found that the degradation decreased from 50 % to 17 % at catalyst concentration of 0,008 % and meanwhile the pH value increasing from 10.7 to 9.5.

The influence of repetitions times on degradation rate and restoration of photocatalytic properties of TiO_2

The surface modified glass beads were immersed in the TiO_2 sol for 10 min. Subsequently, they were dried at 100 °C in a vacuum dryer and calcinated at 550 °C for 2 h. The procedure was repeated until the glass beads were coated with 6 layers of TiO_2. The degradation was conducted at room temperature and degradation time was 120 min with ammonia content about 700 mg / L in wastewater. The same glass beads were reused for 4 cycles to check the degradation efficiencies. Restoration of photocatalytic properties of TiO_2 thin film was executed as following: after reusing for 4 cycles, TiO_2 film coated samples were rinsed with distilled water and dried in the vacuum oven. After that, they were placed in a resistance furnace to calcinate at 550 °C for 2 h. Under the same experimental conditions, the degradation efficiencies were re-measured. The results are presented in Fig. 9.

From the above chart, we can conclude that repetitions result in degradation efficiency reduction to some extent. After 4 cycles of usages, the degradation efficiency of the sample reclined ~34 % comparing to the original value. This implies that the TiO_2 films can be used continuously for water treatment. Fortunately, this study did not find any deposited thin films peeling off from the glass beads.

This can be explained from the perspective of TiO_2 photocatalytic mechanism. Oxidation and decomposition occurred on the surface of TiO_2. After photocatalytic reaction, more or less residuals remained on the surface, which weakened the participation of TiO_2 in the next photocatalytic reactions and therefore resulted in a steady decline in the degradation efficiency. During the restoration process, calcination at 550 °C for 2 h physically removed residuals adsorbed on TiO_2 surface. Restoration of photocatalytic properties of TiO_2 thin film had significant effect and ~93 % efficiency was restored in the recycled sampled in contrast to a new sample as shown on Fig. 9.

Conclusion

This project was undertaken to embed the TiO_2 thin film on the glass beads via a deep coating in a sol–gel

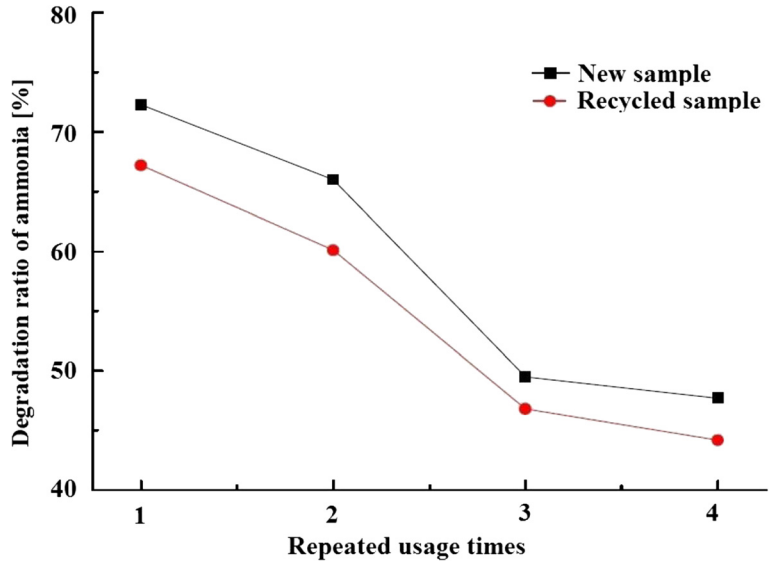

Fig. 9 Influence of repetitions times on degradation rate and restoration efficiency

system and the performance of our lab-scale photocatalytic reactor where the volume of reactant solution is <1 L was evaluated on the basis on change in concentration of high ammonia content with respect to time. Immobilization of TiO_2 on rigid glass beads surface is due to the main advantage that the glass substrate is the transparent even after the immobilization. This allows the penetration of light resulting in improved photocatalysis. Several suggestions on the basis of the results from the trail tests can be summarized, which contributes to the continue research in the future.

At 550 °C, TiO_2 sample presented the highest photocatalytic activity among all counterparts, where the mass fraction on the rutile phase accounted for around 18.87 % in the mixed crystals; the relationship between film thickness and degradation efficiency is worth noticing. The thicker films brought out higher degradation. However, degradation went slower when TiO_2 film was over 6 times of coating; it was observed that the optimum removal rate is obtained at pH 3.4 when aqueous initial pH changed from 1 to 13; the outcomes supported the finding that better degradation rate was achieved for high concentration ammonia in strong acidic or mildly acidic wastewater rather than neutral, mildly alkaline and strongly alkaline conditions; the influence of exposure time of the TiO_2 films under UV irradiation was examined. Within time range of 30 ~ 120 min of UV exposure, the percentage of photo-degradation of the samples increases with irradiation time growth. After 120 min, as time proceeds, the growth of the degradation rate of all samples substantially slowed down and almost unchanged; one of the more significant findings to emerge from this study is that repetitions led to degradation efficiency reduction to some level; after 4-cycles re-utilization, the degradation efficiency reduced ~34 % compared to the original value. However, ~93 % efficiency was restored in the recycled sampled in contrast to a new sample and the TiO_2 thin film could recover its photocatalytic properties effectively.

The photocatalytic degradation treatment in this study has proved to be very effective to removal of high concentration ammonia from its solutions. In addition, this photocatalytic reactor seems to be a simple, energy efficient, eco-friendly, less expensive to build and operate photocatalytic reactor to handle ammonium-rich wastewater. This study provides good reference data for the design of pilot plant-scale reactors for treating ammonium-rich wastewater.

Competing interests

On behalf of all of the co-authors, I declare that I have no significant competing financial, professional or personal interests that might have influenced the performance or presentation of the work described in this manuscript.

Authors' contributions

XG and HW who conducted the experiments, data acquisition and analysis. CY and QL supervised their work. XC participated in background reviewing, correcting and improving English. JH and XG drafted the manuscript. All authors read and approved the final manuscript.

Acknowledgements

This study is funded by the Projects of Education Department of Sichuan Province (14CZ0004), China.

Author details

[1]The College of Chemistry and Materials Science, Sichuan Normal University, Chengdu, China. [2]The Electrical Engineering College, Guizhou University, Guizhou, China. [3]Institute of Thermal Engineering, University of Applied Sciences and Arts of Western Switzerland, Yverdon-les-Bains, Switzerland.

Received: 3 November 2015 Accepted: 26 November 2015
Published online: 07 December 2015

References

1. Aguilar JB, Orban P, Dassargues A, Brouyère S (2007) Identification of groundwater quality trends in a chalk aquifer threatened by intensive agriculture in Belgium. Hydrogeology J 15(8):1615–1627
2. Alonso A, Camargo JA (2003) Short-term toxicity of ammonia, nitrite, and nitrate to the aquatic snail Potamopyrgus antipodarum (Hydrobiidae, Mollusca). Bull Environ Contam Toxicol 70:1006–1012
3. Alonso A, Camargo JA (2004) Toxic effects of unionized ammonia on survival and feeding activity of the freshwater amphipod Eulimnogammarus toletanus (Gammaridae, Crustacea). Bull Environ Contam Toxicol 72:1052–1058
4. Ammonia. Geneva (1986) World Health Organization, (Environmental Health Criteria, No. 54)
5. AWWA (American Water Works Association) (2000) Water quality and treatment, A handbook of Community Water Supplies, Fifth Editionth edn. Mc Graw Hill Co, New York
6. Bahnemann D (2004) Photocatalytic water treatment: solar energy applications. Solar Energy 77:445–459
7. Bahnemann DW, Cunningham J, Fox MA, Pelizzetti E, Pichat P, Serpone N, Zepp RG, Heltz GR (1994) Aquatic Surface Photochemistry. Lewis Publishers, Boca Raton, p 261
8. Batzill M, Morales EH, Diebold U (2006) Influence Of Nitrogen Doping On The Defect Formation and Surface Properties of TiO2 Rutile And Anatase. Phys Rev Lett 96:26103
9. Blanco-Galvez J, Fernández-Ibáñez P, Malato-Rodríguez S (2007) Solar Photocatalytic Detoxification and Disinfection of Water: Recent overview. J Solar Energy Eng 129:4–15
10. Carp O, Huisman C, Reller A (2004) Photoinduced reactivity of titanium dioxide. Prog Solid State Chem 32:33–177
11. Coronado DR, Gattorno GR, Pesqueira ME, Cab C, Coss R, Oskam RG (2008) Phase pure TiO_2 nanoparticles: anatase, brookite and rutile. Nanotechnology 19:145605
12. Dieter HH, Möller R (1991) Ammonium. In: Aurand K (ed) Die Trinkwasser verordnung, Einführung und Erläuterungen. [The drinking-water regulations, introduction and explanations]. Erich-Schmidt Verlag, Berlin, pp 362–368
13. Ding K, Miao Z, Hu B, An G, Sun Z, Han B, Liu Z (2010) Study on the anatase to rutile phase transformation and controlled synthesis of rutile nanocrystals with the assistance of ionic liquid. Langmuir 26:10294–10302
14. Ding S, Wang L, Ding Y, Zhang M, Wang Z (2006) Microwave Synthesis and Photocatalysis of Nano-TiO2 Mix-crystals. Chinese J Appl Chem 23:6
15. Frank SN, Bard AJ (1977) Heterogeneous photocatalytic oxidation of cyanide ion in aqueous solutions at titanium dioxide powder. J Am Chem Soc 99:303–304
16. Frank SN, Bard AJ (1977) Heterogeneous photocatalytic oxidation of cyanide and sulfite in aqueous solutions at semiconductor powders. J Phys Chem 81:1484–1488
17. Fujishima A, Zhang X, Tryk D (2008) TiO2 photocatalysis and related surface phenomena. Surf Sci Rep 63:515–582
18. Gaya UI , Abdullah AH (2008) Heterogeneous photocatalytic degradation of organic contaminants over titanium dioxide: A review of fundamentals, progress and problems. J Photochem Photobiol C: Photochem Rev 9(1):1–12
19. Hasan MM, Haseeb ASMA, Saidur R, Masjuki HH (2009) Effect of annealing treatment on optical properties of Anatase TiO2 thin films. World Acad Sci, Eng Technol 40:221–225, ISSN 2010-376X
20. Hirakawa T, Yawata K, Nosaka Y (2007) Photocatalytic reactivity for O2•− and •OH radical formation in anatase and rutile TiO2 suspension as the effect of H2O2 addition. Appl Catal A 325:105–111
21. Hurum Deanna C, Agrios Alexander G, Gray Kimberly A, Rajh T, Thurnauer Marion C (2003) Explaining the Enhanced Photocatalytic Activity of Degussa P25 Mixed-Phase TiO2 Using EPR. J Phys Chem B 107(19):4545–4549
22. Ji Chenjing, Zhang Yanfeng, Wei Yu (2010) Microwave Assisted Synthesis and Photocatalysis Property of Nanometer Titania Journal of Hebei Normal University (Natural Science Edition), Vol. 34, No.5
23. Jiang Y, Somers G (2009) Modeling effects of nitrate from non-point sources on groundwater quality in an agricultural watershed in Prince Edward Island, Canada. Hydrogeology J 17(3):707–724
24. Jin L, Dai B (2012) TiO2 activation using acid-treated vermiculite as a support: Characteristics and photoreactivity. Appl Surf Sci 258:3386–3392
25. Jin YS, Kim KH, Park SJ, Yoon HH, Choi HW (2010) Properties of TiO2 Films Prepared for Use in Dye-sensitized Solar Cells by Using the Sol-gel Method at Different Catalyst Concentrations. J Korean Physical Society 57(4):1049–1053. doi:10.3938/jkps.57.1049
26. Kim, D.J., Hahn, S.H., Oh, S.H., Kim, E.J., Materials Letters (2002) Influence of calcination temperature on structural and optical properties of TiO2 thin films prepared by sol–gel dip coating, Volume 57, Issue 2, Pages 355–360
27. Lee DK (2003) Mechanism and Kinetics of the Catalytic Oxidation of Aqueous Ammonia to Molecular Nitrogen. Environ Sci Technol 37:5745–5749
28. Li W, Ni C, Lin H, Huang CP, Shah SI (2004) Size dependence of thermal stability of TiO2 nanoparticles. J Appl Phys 96:6663–6668
29. Li X, Liu L, Yang F, Zhang X, Barford J (2006) Nitrogen Removal via Coupled Ammonia Oxidation and Nitrite Reduction Using Pt/TiO2 and Photocatalysis. Chinese J Inorg Chem 22(7):1180–1186, ISSN: 1001-4861
30. Madras G, McCoy BJ, Navrotsky A (2007) Kinetic model for TiO2 polymorphic transformation from anatase to rutile. J Am Ceram Soc 90:250–255
31. Minero C, Maurino V, Vione D (2013) Photocatalytic mechanisms and reaction pathways drawn from kinetic and probe molecules. In: Pichat P (ed) Photocatalysis and Water Purification: From Fundamentals to Recent Applications, 1st edn. Wiley-VCH, Weinheim, Germany, pp 53–72
32. Mojie S, Chao Y, Chong Z, Chuangjie Z (2012) Influence of TiO2 /PVDF Membrane Catalyzed Ozonation of Ammonia Wastewater, Proceedings of the 2011 International Conference on Informatics, Cybernetics, and Computer Engineering (ICCE2011) November 19–20, 2011, vol 112. Advances in Intelligent and Soft Computing, Melbourne, Australia, pp 771–778
33. Mukhopadhay A, Akber A, Al-Awadi E (2011) Evaluation of urban groundwater contamination from sewage network in Kuwait City. Water Air Soil Pollut 216(1–4):125–139
34. Murgia SM, Poletti A, Selvaggi R (2005) Photocatalytic degradation of high ammonia concentration water solutions by TiO2. Ann Chim 95(5):335–343
35. Ngo Michel J, Gujisaite V, Latifi A, Simonnot MO (2014) Parameters describing nonequilibrium transport of polycyclic aromatic hydrocarbons through contaminated soil columns: estimability analysis, correlation, and optimization. J Contam Hydrol 158:93–109
36. Nosaka Y, Nosaka AY (2013) Identification and roles of the active species generated on various photocatalysts. In: Pichat P (ed) Photocatalysis and Water Purification: From Fundamentals to recentApplications, 1st edn. Wiley-VCH, Weinheim, Germany, pp 3–24
37. Ollis DF, Pelizzetti E, Serpone N (1991) Photocatalyzed destruction of water contaminants. Environ Sci Tech 25:1522–1529
38. Paola AD, Cufalo G, Addamo M, Bellardita M, Campostrini R, Ischia M, Ceccato R, Palmisano L (2008) Photocatalytic activity of nanocrystalline TiO2 (brookite, rutile and brookite-based) powders prepared by thermohydrolysis of TiCl4 in aqueous chloride solutions. Colloids Surf A 317:366–376
39. Porter JF, Li YG, Chan CK (1999) The effect of calcination on the microstructural characteristics and photoreactivity of Degussa P-25 TiO2. J Mater Sci 34:1523–1531
40. Poulios I, Tsachpinis I (1999) Photodegradation of the textile dye reactive black 5 in the presence of semiconducting oxides. J Chem Technol Biotechnol 71:349–357
41. Prajapati, Jignasha C., Syed, Huma S., Chauhan, Jagdiah (2014) Removal of Ammonia from wastewater by ion exchange technology, Int J Innovative Res Techno, Volume 1 Issue 9
42. Rao GT, Rao VVSG, Ranganathan K, Surinaidu L, Mahesh J, Ramesh G (2011) Assessment of groundwater contamination from a hazardous dump site in Ranipet, Tamil Nadu, India. Hydrogeology J 19(8):1587–1598
43. Scotti R, Bellobono IR, Canevali C, Cannas C, Catti M, D'Arienzo M, Musinu A, Polizzi S, Sommariva M, Testino A, Morazzoni F (2008) Sol–gel pure and mixed phase titanium dioxide for photocatalytic purposes: relations between phase composition, catalytic activity, and charge-trapped sites. Chem Mater 20:4051–4061
44. Shan AY, Ghazi TIM, Rashid SA (2010) Immobilisation of titanium dioxide onto supporting materials in heterogeneous photocatalysis: A review. Appl Catal A 389:1–8
45. Spurr RA, Myers H (1957) Quantitative analysis of anatase-rutile mixtures with an X-ray diffractomer. Anal Chem 29(5):760–762
46. Stamatis G, Parpodis K, Filintas A, Zagana E (2011) Groundwater quality, nitrate pollution and irrigation environmental management in the Neogene sediments of an agricultural region in central Thessaly (Greece). Environ Earth Sci 64(4):1081–1105
47. Stathatos E, Papoulis D, Aggelopoulos CA, Panagiotaras D, Nikolopoulou A (2012) TiO2/palygorskite composite nanocrystalline films prepared by surfactant templating route: Synergistic effect to the photocatalytic degradation of an azo-dye in water. J Hazard Mater 211:68–76

48. Sun Y, Guo W, Shan Y, Lv H, Song Y (2011) Treatment of ammonia nitrogen wastewater from coal gasification process with TiO_2 photocatalysts doped with metal ions. Ind Water Treat 31:9
49. Suzana M, Francisco P, Mastelaro VR (2002) Inhibition of the Anatase Rutile Phase Transformation with Addition of CeO2 to CuO-TiO2 System: Raman Spectroscopy, X-ray Diffraction, and Textural Studies. Chem Mater 14:2514
50. Vijay R, Khobragade P, Mohapatra PK (2011) Assessment of groundwater quality in Puri City, India: an impact of anthropogenic activities. Environ Monit Assess 177(1–4):409–418
51. Wang SJ, Ma J, Yang YX, Zhang J, Qin QD, Liang T (2007) Influence of nanosized TiO2 catalyzed ozonation on the ammonia concentration in Songhua River water. Huan Jing Ke Xue 28(11):2520–2525, PMID:18290476
52. Zainovia L, Chin Hui K, Srimala S (2009) Effect Of Annealing Temperature on The Anatase and rutile Tio2 nanotubes formation. J Nucl Related Technol 6:1
53. Zhang J, Nosaka Y (2014) Mechanism of the OH radical generation in photocatalysis with TiO2 of different crystalline types. J Phys Chem C 118: 10824–10832
54. Zhu B, Zou L (2009) Trapping and decomposing of color compounds from recycled water by TiO2 coated activated carbon. J Environ Manag 90:3217–3225
55. Zhu J, Yang J, Zhen-Fen B, Ren J, Yong-Mei L, Cao Y, He-Xing et al (2007) Nanocrystalline anatase TiO2 photocatalysts prepared via a facile low temperature nonhydrolytic sol-gel reaction of TiCl4 and benzyl alcohol. Appl Catal B-Environ 76(1–2):82–91